JOURNAL OF GEOPHYSICAL RESEARCH, VOL. 97, NO. A12, PAGES 19,403–19,412, DECEMBER 1, 1992

# The Quiet Time Polar Cap: DE 1 Observations and Conceptual Model

J. L. BURCH,[1] N. A. SAFLEKOS,[2] D. A. GURNETT,[3] J. D. CRAVEN,[4] AND L. A. FRANK[3]

Auroral activity increases over the polar caps during quiet times, which are associated with northward interplanetary magnetic field (IMF) components. Polar cap auroras (Sun-aligned arcs, theta auroras, and horse collar auroras) occur under these conditions. DE 1 data show that the theta and horse collar auroras are generally characterized by sunward convection, closed field lines, auroral hiss, and inverted-V events. These phenomena are similar to those observed along the auroral oval but have somewhat lower electron energies. Adjacent dark regions of the polar caps appear to contain open field lines and antisunward convection. A conceptual northward IMF merging model containing lobe cells, merging cells, and viscous cells is shown to be consistent with the observations. As the IMF becomes more northward, the polar arc configuration changes from the "horse collar" pattern to the theta aurora pattern in the model, and this is shown to be generally true for the set of published data on these phenomena. The model involves dayside merging both at high latitudes on open field lines and at lower latitudes on closed field lines. The ratio between the merged flux produced by the high-latitude merging to that produced by the lower-latitude merging increases as the IMF becomes more northward. Two types of open field lines, equator-crossing and non-equator-crossing, are produced by the higher- and lower-latitude merging, respectively. The equator-crossing field lines have a strong azimuthal component of convection as they flow around the magnetopause, while the non-equator-crossing field lines can convect more or less directly across the polar cap, leading to an antisunward flow channel across the central polar cap. This antisunward flow region grows as the IMF becomes less northward, causing dual polar cap arcs to spread out into the horse collar configuration. The sunward flow segments of the lobe cells are associated with induced electric fields, thus accounting for the particle energization leading to auroral forms.

## INTRODUCTION

One of the fundamental problems of magnetospheric physics is the nature of the solar wind/magnetosphere interaction for various orientations of the interplanetary magnetic field (IMF). Although most of our basic concepts about an open magnetosphere are based on observations and expectations related to southward IMF conditions, data from extremely quiet times when the IMF is generally northward have suggested a fundamentally different mode of interaction. During these periods, auroral activity subsides along the auroral ovals but increases over the polar caps, which contain Sun-aligned auroral arcs [*Lassen*, 1979], theta auroras [*Frank et al.*, 1986], or horse collar auroras [*Hones et al.*, 1989], and large zones of sunward convection [*Burke et al.*, 1979]. Recent studies have shown that the well-known region 1 and 2 current systems can disappear during extremely quiet periods with northward IMF [*Rich and Gussenhoven*, 1987] and that the usually organized polar cap convection pattern sometimes relaxes to a state of small-scale convection eddies [*Hoffman et al.*, 1988]. There has also been considerable discussion about whether a four-cell convection pattern or a distorted two-cell convection pattern occurs in the polar cap at these times [*Zhu and Kan*, 1990]. A three-cell type pattern could also appear as an intermediate state [*Blomberg and Marklund*, 1991].

In this paper we will refer to the polar cap as the region poleward of the main auroral oval. We shall see that particularly for northward IMF conditions the polar cap defined in this way can contain regions of both open and closed magnetic field lines and both sunward and antisunward convection. The term polar arcs will be used in a general sense to denote both "theta auroras" and "horse collar" (equivalent to "teardrop") auroras, as well as individual Sun-aligned polar cap arcs that belong to neither of these two categories. As demonstrated by *Elphinstone et al.* [1990], significantly different patterns of the teardrop-shaped horse collar auroras occur as functions of the IMF, but these are all placed in a single category in this paper.

In this study we examine the characteristics of polar cap plasmas and waves during a quiet period with an IMF that is northward (although an IMF data gap existed during part of the period) when multiple adjacent regions of sunward and antisunward convection were observed by Dynamics Explorer 1 (DE 1). The sunward convection regions contained inverted-V events and lower total plasma densities. DE 1 auroral images show the appearance of "horse collar" auroras [*Hones et al.*, 1989] during this time, with crossing of the duskside branch of the "horse collar" coinciding with one of the sunward convection cells. More intense plasma wave emissions (auroral hiss) were also observed in the sunward flow regions at the highest invariant latitudes (>85°), while at somewhat lower latitudes, associated with the main auroral oval, strong bidirectional field-aligned currents and intense ELF and VLF wave activity occurred in both sunward and antisunward convection zones. Similar phenomena were reported by *Frank et al.* [1986] in association with theta auroras. We will show that while both theta auroras and horse collar auroras occur during northward

[1]Instrumentation and Space Research Division, Southwest Research Institute, San Antonio, Texas.
[2]Division of Earth and Physical Sciences, University of Texas at San Antonio.
[3]Department of Physics and Astronomy, University of Iowa, Iowa City.
[4]Geophysical Institute and Department of Physics, University of Alaska, Fairbanks.

Copyright 1992 by the American Geophysical Union.

Paper number 92JA01537.
0148-0227/92/92JA-01537$05.00

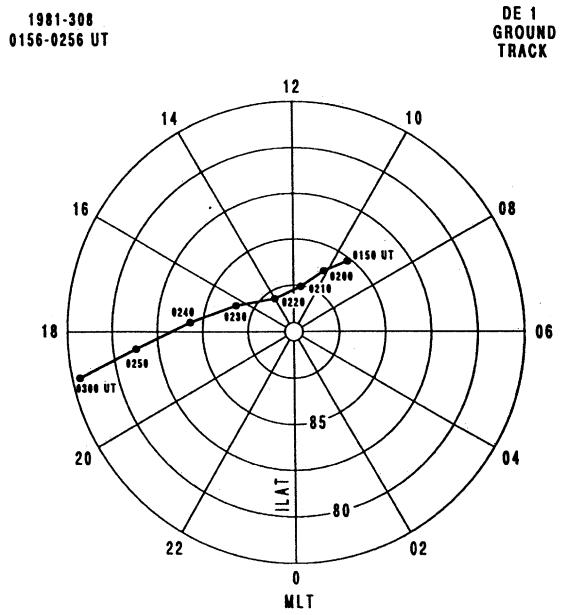


Fig. 1. Polar plot showing the DE 1 ground track in MLT versus ILAT, covering the interval 0155–0300 UT on November 4, 1981 (day 81308).

IMF, the theta auroras tend to be associated with much larger IMF $+B_z$ components and particularly with larger values of IMF magnitude.

To explain these observations, we present a conceptual merging model of the magnetosphere, which involves open flux tubes in the antisunward convection regions of the polar cap and reconnected closed flux tubes in the sunward convection regions of the polar cap, accounting for the auroral plasma and wave activity observed there. The resulting convection cells that remain totally within the polar cap would be classified as lobe cells in the model of *Burch et al.* [1985]. The model also includes merging cells, which involve open flux tubes convecting more or less directly over the polar cap with the return convection occurring at lower latitudes within or equatorward of the auroral oval on closed flux tubes [e.g., *Burch et al.*, 1985]. The fraction of the polar cap covered by merging cells is relatively small for northward IMF conditions, becoming almost vanishingly small for strongly northward IMF. This IMF dependence leads in this model to horse collar auroras and theta auroras for weakly northward IMF and strongly northward IMF, respectively. At lower latitudes in the auroral oval, closed field line convection would be driven by viscous processes.

## OBSERVATIONS

Figure 1 shows the DE 1 ground track in magnetic local time (MLT) and invariant latitude (ILAT) for about a 1-hour interval on November 4, 1981 (day 81308), when DE 1 was in the polar cap. Figure 2 shows ISEE 1 IMF data, which contain some gaps during the period of interest but show a northward IMF before and during the first part of the DE 1 observations. With the additional evidence that the *AE* index remained below 20 nT for the first 5 hours of the day, we infer that the IMF was mostly northward during the entire period of day 81308 plotted in Figure 1.

Plate 1 is a joint presentation of PWI (plasma wave instrument) and HAPI (high-altitude plasma instrument) measurements. The top panel is a frequency-time spectrogram of PWI electric field spectral density covering the same time period as Figure 1. The frequency range is from 10 Hz to 50 kHz; the upper and lower black curves represent the proton and electron gyrofrequencies, respectively. For this particular pass the magnetic field spectrogram (not shown) does not indicate the presence of any significant spectral densities except near 0240, 0250, and 0255 UT, so we may consider most of these waves to be electrostatic. The clear cutoff frequencies of the auroral hiss (near $10^4$ Hz) can be used to estimate the plasma frequency ($f_{pe}$), from which the total plasma density ($n_e$) can be obtained.

In the second panel are plotted the number flux derived from the HAPI suprathermal electron data and the total plasma density derived from the plasma frequency. The electron number flux is computed over the energy range from 25 eV to 31 keV in order to avoid a contribution from lower-energy spacecraft photoelectrons. In most cases the total number density increases when the number flux of suprathermal electrons decreases. In the third panel of Plate 1 we plot the PWI convection electric field component along the spacecraft velocity vector and perpendicular to **B** (red line) along with field-aligned currents computed from the electron data (green line). There is an excellent anticorrelation between the electric field ($E_\perp$) and the number flux. When the dc electric field is positive (along the spacecraft velocity vector), it corresponds to antisunward convection. Referring back to the wave spectrogram, it seems that before 0240 UT the broadband electric field noise at frequencies below a few hundred hertz intensifies significantly in regions

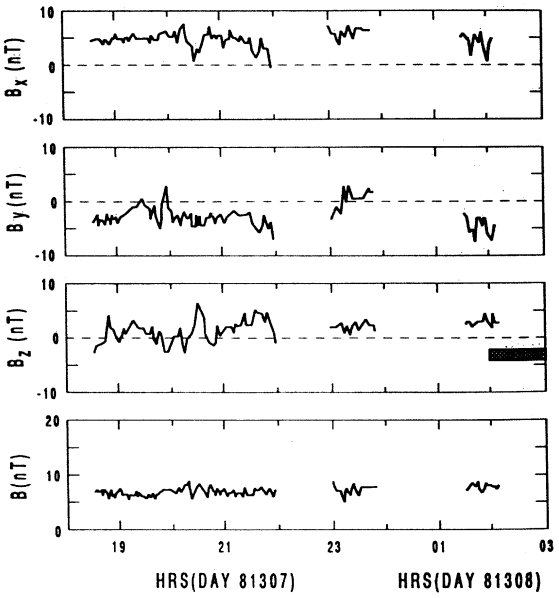


Fig. 2. ISEE 1 IMF data in GSM coordinates for November 3–4, 1981. The ISEE 1 spacecraft position in GSM coordinates was approximately $x = 19.4\ R_E$, $y = -11.0\ R_E$, $z = -2.5\ R_E$.

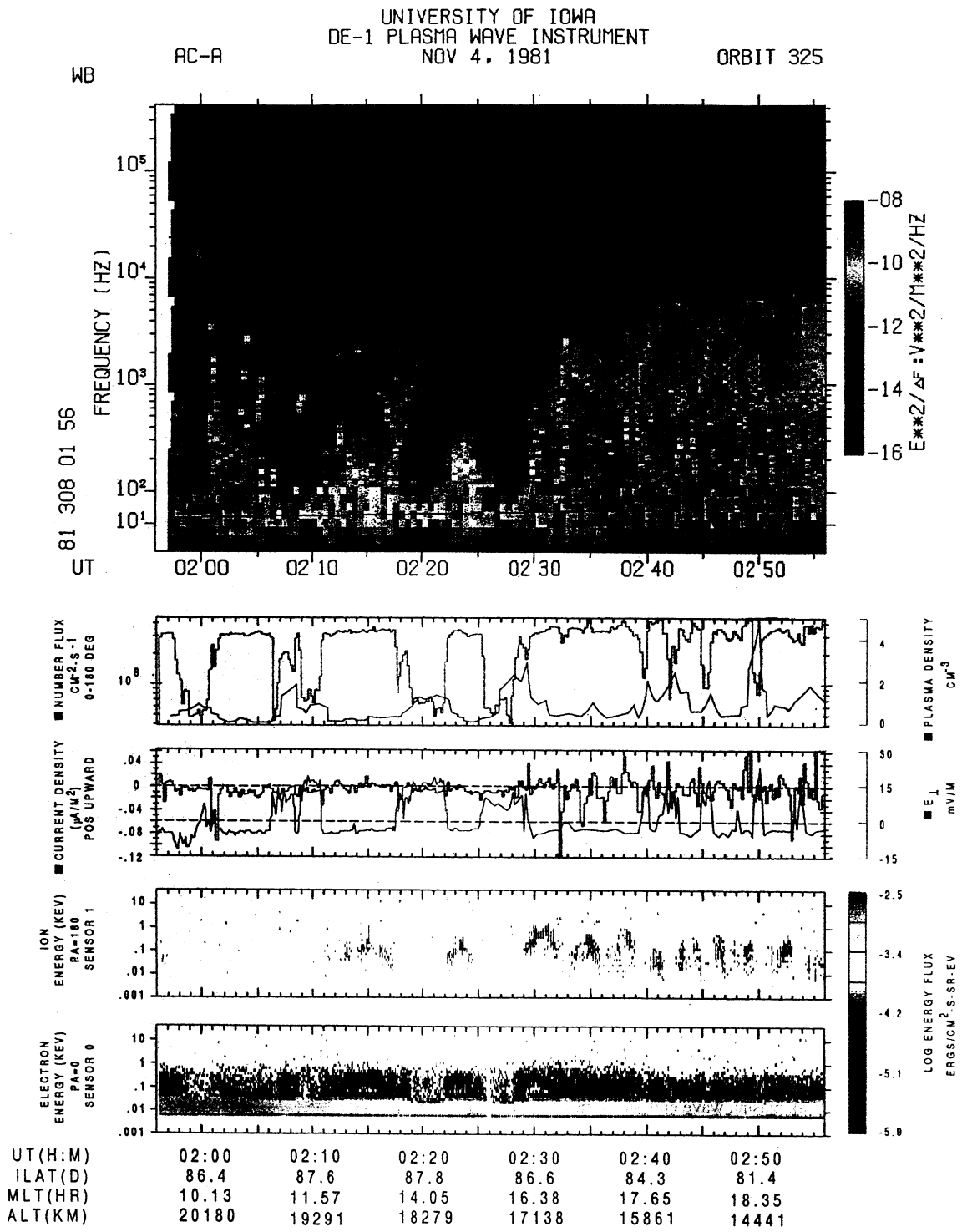


Plate 1. Joint presentation of PWI and HAPI measurements. Top panel shows the electric component of ELF/VLF waves from 10 Hz to 50 kHz, and the Cartesian plots below (in red) show the PWI convection electric field $E_\perp$ and the total plasma density inferred from the wave data. The number flux and current density from HAPI are shown in green. The bottom two color spectrograms show the ion and electron energy fluxes. The ion fluxes are for upward moving ions (pitch angle 165°–180°), and the electron fluxes are for downward moving electrons (pitch angle 0°–15°).

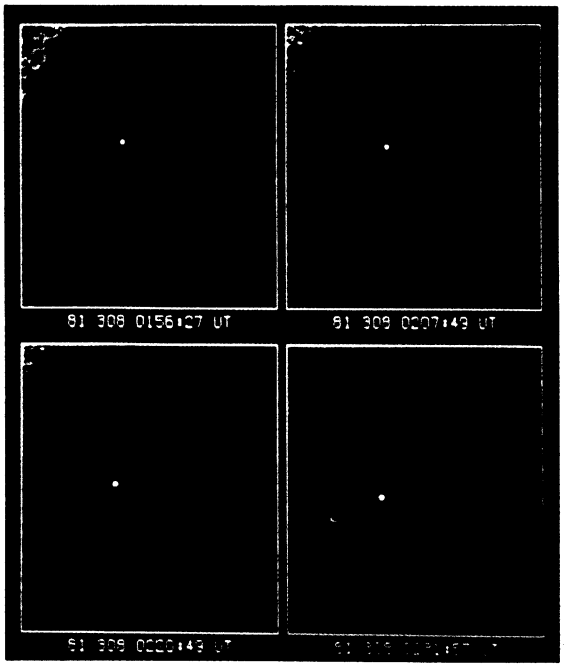


Plate 2. DE 1 ultraviolet auroral images in the northern hemisphere for the time interval 0150–0238 UT on November 4, 1981. The position of DE 1 at the specified UT in each image is mapped along the magnetic field to auroral altitudes and is indicated by a white dot. This "footprint" of the magnetic field line is scanned by the auroral imager at the specified time.

Although strikingly different characteristics of the sunward and antisunward convection regimes are consistently observed, the additional information provided by global auroral images is essential in relating them to magnetospheric structure and the effects of the IMF. Plate 2 shows auroral-oval-centered sections obtained from four consecutive auroral images (at wavelengths from 123 to 160 nm) in the northern hemisphere for the time interval 0150–0238 UT on November 4, 1981. The position of DE 1 mapped along magnetic field lines to auroral altitudes is indicated by a white dot in each image, and the UT at which the "foot" of the DE 1 field line was sampled is given below the image. The sequence of images continues in Plate 3, in which the four images span the time interval 0238–0327 UT. The auroral distributions seen in the bottom two images in Plate 2 and those in Plate 3 are reasonably similar to the horse collar aurora described by *Hones et al.* [1989] as well as to the auroral topology associated with northward IMF by *Elphinstone et al.* [1990]. Lack of a more detailed agreement with the outstanding example and idealized illustration provided by *Hones et al.* [1989] is due in large part to the reduced brightness of the aurora in this example. With these images at hand, it appears likely that the multiple zones of sunward convection shown in Plate 1 are associated with multiple encounters with the duskside polar arc of the horse collar auroral configuration or else with multiple duskside polar arcs in the same general region. It is not possible to identify uniquely the arc or arcs that were encountered, because of the formation, disappearance, and motion of arcs that may occur during the 12 min required to construct each image shown in Plates 2 and 3. However, as one example of how a prominent auroral feature in the images can be

of sunward convection (negative $E_\perp$) and higher suprathermal electron number flux.

Below the convection electric field plot we show the ion upward energy fluxes in energy-time spectrogram format. They all appear as inverted V's, which without exception occur in regions of sunward convection (negative $E_\perp$). Below the ion plots the electron downward energy fluxes are shown. The weak electron inverted-V events associated with the much more energetic upward ion inverted V's indicate that most of the particle acceleration was occurring below the spacecraft. As noted above, decreases of total plasma density accompany these events, calling to mind the density cavities observed at mid-altitudes above the auroral oval [*Persoon et al.*, 1988]. Between the inverted-V events, only weak polar rain electron fluxes are present in the spectrogram in the bottom panel of Plate 1.

In summary, the regions of antisunward convection in Plate 1 contain weak plasma wave emissions, no inverted-V events, somewhat higher total plasma densities, and much lower suprathermal electron densities as compared to the sunward convection zones, which contain intense auroral hiss emissions and inverted-V events with maximum energies of about 1 keV. The typical polar rain electron fluxes in the antisunward flow regions (e.g., from 0218 to 0222 UT in Plate 1) are suggestive of an open field line topology [*Fairfield and Scudder*, 1985], while the higher total plasma densities in those regions are consistent with the convection of plasma from the cusp ion fountain [*Lockwood et al.*, 1985].

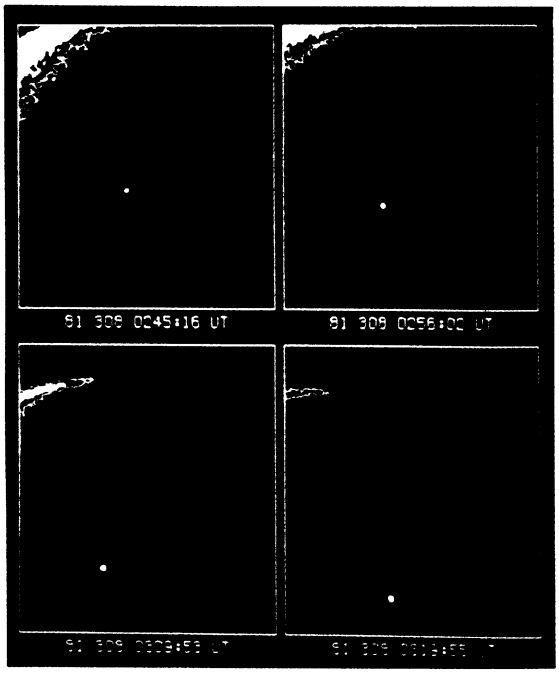


Plate 3. Same as Plate 2 except for the time interval 0238–0327 UT.

TABLE 1. Polar Arc Observations

| Type | Imaging Spacecraft | Date | Observation Time or Period (UT) | IMF Spacecraft | $\langle B_z \rangle$, nT | $\langle B \rangle$, nT | Reference |
|---|---|---|---|---|---|---|---|
| Horse collar | ISIS 2 | Feb. 20, 1974 (74051) | 0545 | IMP 8 | 3.65 | 4.04 | *Murphree et al.* [1982] |
| Theta | DE 1 | Oct. 17, 1981 (81290) | 1431–1657 | ISEE 3 | 8.78 | 16.05 | *Frank et al.* [1986] |
| Theta | DE 1 | Oct. 31, 1981 (81304) | 2315–2339 | IMP 8 | 2.35 | 6.58 | *Frank et al.* [1986] |
| Horse collar | DE 1 | Nov. 4, 1981 (81308) | 0150–0327 | ISEE 1 | 3.00 | 7.07 | this paper |
| Theta | DE 1 | Nov. 8, 1981 (81312) | 1234–1601 | ISEE 3 | 13.38 | 16.50 | *Frank et al.* [1986] |
| Horse collar | DE 1 | Nov. 13, 1981 (81317) | 1856–1955 | ISEE 1 and IMP 8 | 4.00 | 9.90 | *Bim et al.* [1991] |
| Theta | DE 1 | Nov. 25, 1981 (81329) | 1144–1232 | ISEE 3 | 12.81 | 28.15 | *Frank et al.* [1986] |
| Theta | DE 1 | Jan. 21, 1982 (82021) | 2008–2109 | ISEE 3 | 4.69 | 20.22 | *Nielson et al.* [1990] |
| Horse collar | DE 1 | May 9, 1983 (83129) | 0823–1007 | IMP 8 | 1.67 | 6.50 | *Hones et al.* [1989] |
| Theta | DE 1 and Viking | Aug. 3, 1986 (86215) | 1800–1926 | IMP 8 | 6.55 | 10.81 | *Craven et al.* [1991] |
| Horse collar | Viking | Sept. 23, 1986 (86266) | 1208:39 | IMP 8 | 1.76 | 7.36 | *Elphinstone et al.* [1990] |
| Theta | Viking | Sept. 25, 1986 (86268) | 2052–2104 | IMP 8 | 3.35 | 5.99 | *Obara et al.* [1988] |

Average value of IMF $B_z$ and $B$ were computed over the time interval from 1 hour before the start of the observation period until the end of the period. A 1-hour time delay was assumed in this case of ISEE 3 IMF data. Read 74051 as day 51 of 1974.

identified clearly in the energy-time spectrograms of Plate 1, consider the last image of Plate 2. Here the magnetic "footprint" of DE 1 was scanned by the imager at 0231:57 UT, just as DE 1 appeared to intercept the duskside polar arc of the horse collar aurora. This interception is confirmed by the plasma observations through the detection of an inverted-V event at DE 1 altitudes in the overlapping time interval 0229–0232 UT.

## CONCEPTUAL MODEL

The observations discussed in the previous section were obtained during an extremely quiet period ($AE \leq 20$ nT) with rather small northward IMF components. Numerous other cases showing similar plasma and field behavior have been observed in the DE 1 data and are now being analyzed on a statistical basis. All occurred during northward IMF conditions. Common features of all of these cases are as follows: (1) multiple zones of sunward and antisunward convection occur at $\Lambda > 80°$ in the polar cap; (2) the sunward flow regions contain inverted-V events, auroral hiss, and density cavities that are very similar to phenomena normally associated with the nightside auroral oval; and (3) the antisunward flow regions contain very weak wave activity, no inverted-V events, higher total plasma densities, and weak, unaccelerated polar rain electron distributions. We conclude that the antisunward flow is on open field lines while the sunward flow is on closed field lines, although a unique identification of each inverted-V event with a particular polar arc cannot be made because of the 12-min time resolution of the auroral images. Most of these characteristics have previously been noted by *Frank et al.* [1986] in connection with observations of theta auroras, which were also observed to occur in the sunward flow regions. In the example presented here the global auroral images are consistent with the general description of horse collar auroras [*Hones et al.*, 1989], so a proposed model could in principle address both the theta and the horse collar auroral configurations since they occur during similar conditions.

Several models have been proposed to explain the behavior of polar cap plasma convection during quiet, northward IMF conditions [e.g., *Maezawa*, 1976; *Frank et al.*, 1982; *Zanetti et al.*, 1984; *Reiff and Burch*, 1985; *Kan and Burke*, 1985; *Israelevich*, 1990; *Jankowska et al.*, 1990]. *Kan and Burke* [1985] and *Reiff and Burch* [1985] both explored the consequences of the merging of northward IMF field lines with closed field lines at the dayside polar cap boundary and subsequent reconnection on the nightside between open field lines connected to the northern and southern hemispheres.

The concept of lobe cells was used by *Burch et al.* [1985] to explain convection patterns observed by DE 1 for IMF $B_z$ negative conditions. These cells were described as remaining completely within the polar caps. In a companion paper, *Reiff and Burch* [1985] applied the antiparallel merging hypothesis of *Crooker* [1979] to generalize their convection model to arbitrary IMF directions. Reiff and Burch noted, as others had before, that merging should occur between the IMF and either open or closed tail lobe field lines and that for large $B_x$ and small positive $B_z$, merging should occur primarily in one hemisphere with nearly stagnant convection in the other hemisphere.

In this study some further aspects of the northward $B_z$ convection cells are considered in light of the new DE 1 observations and recent reports on the occurrence of polar arcs. Table 1 lists a number of time periods during which

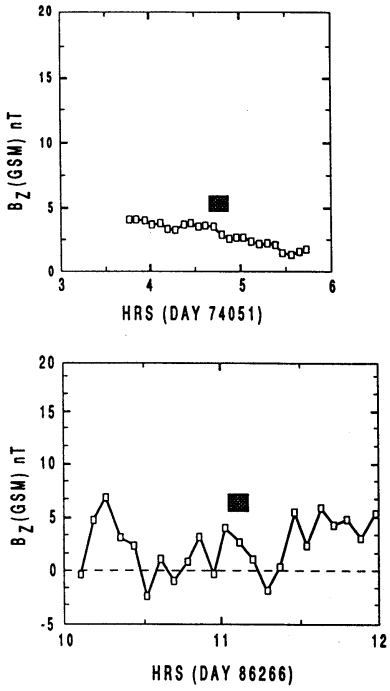


Fig. 3. Five-minute averages of IMF $B_z$ with shaded bars showing times of observation of horse collar auroras.

polar arcs describable as either theta auroras [*Frank et al.*, 1986] or horse collar auroras [*Hones et al.*, 1989] were observed by imagers on the ISIS 2, DE 1, or Viking spacecraft. The example discussed above appears in Table 1 as the fourth entry. Recalling from Figure 2 that that example was a horse collar aurora with a weak (≤5 nT) northward IMF, we show in Figure 3 plots of IMF $B_z$ for two of the other horse collar aurora events in Table 1 (the first and eleventh entries). In Figure 3 the periods of observation of horse collar auroras are shown by shaded bars. Since the IMF observations were made by IMP 8 and thus within 35 $R_E$ geocentric distance, no transit time correction is shown. As in Figure 2, both cases shown in Figure 3 occurred for weak (≤5 nT) northward IMF conditions.

Figure 4 shows IMF data for four of the theta aurora cases listed in Table 1. Again the times of observation of the theta arcs are shown by shaded bars, which are shifted 1 hour earlier for these cases in which ISEE 3 IMF data are used in order to take the typical delay time from ISEE 3 into account. Each of the four theta aurora cases shown in Figure 4 is associated with IMF $B_z$ values that reach rather high values between 10 and 30 nT. In Table 1, average IMF data for each of the polar aurora observations from either ISEE 1, ISEE 3, or IMP 8 are listed, with the average values of $B$ and $B_z$ computed over the time period from 1 hour before the auroral observations until the end of the observations. The typical 1-hour delay time between the measurement of IMF features at ISEE 3 and their arrival at the magnetosphere was allowed for in computation of the ISEE 3 averages. While it is clear from Table 1 that both horse collar and theta auroras can occur for similar conditions of IMF northward, there is a tendency for the theta auroras to be associated with the largest values of IMF $B_z$ and $B$. This tendency is shown graphically in Figure 5, which is a scatterplot of the IMF $B_z$ and $B$ average values from Table 1 for horse collar and theta aurora observations. While the two types of auroral configurations can occur for similar values of $B_z$ and $B$, the much larger values of these parameters are clearly associated with the theta arcs. We make use of this tendency in constructing a conceptual northward IMF merging model.

Consider the topology of a merging model of the magnetosphere for a nearly due northward IMF. Merging will occur with high efficiency just poleward of both cusps along the first swept-back field lines whether they are open or closed. An individual IMF field line may merge in both hemispheres [*Dungey*, 1961], but in the most general case, merging would only occur in one hemisphere at a time. Several models involving merging with due-northward IMF have been presented before [*Maezawa*, 1976; *Reiff and Burch*, 1985; *Kan and Burke*, 1985]. One important aspect of these models is that unlike for southward IMF merging models, the merged, open field lines cross the equatorial plane, so that these field lines could be misinterpreted as being closed if the definition of closed field lines was that they simply crossed the equatorial plane [e.g., *Birn et al.*, 1991]. Another important feature of the northward IMF merged, open field lines is that they are not likely to convect directly over the polar caps. Because they cross the equatorial plane, their convection must possess a significant azimuthal component. Penetration of the magnetosheath plasma on the newly merged field line into the boundary layer via an interchange instability [*Song and Russell*, 1992] is also a possibility in the case of strongly northward IMF.

At some point downstream of the Earth the open, equator-crossing field lines must reconnect and begin moving toward the Earth just as the non-equator-crossing open field lines must do. Because the tangential stresses on open field lines are greater than those on field lines that remain closed, the newly reconnected (i.e., newly closed) field lines will extend downstream of the boundary of the continuously closed field region of the magnetosphere, which is convecting solely as a result of viscous forces. Thus the earthward motion of the newly reconnected field lines cannot properly be considered as convection, but rather as a large-scale magnetic field reconfiguration involving significant induced electric fields. Such phenomena have been invoked by *Delcourt et al.* [1990] to compute particle energization associated with substorm reconnection in the magnetotail resulting from the induced electric fields associated with substorm reconfiguration of magnetotail topology. We are suggesting here that a similar reconfiguration and induced electric fields occur for the northward IMF merging model but that these phenomena and their effects remain wholly within the polar cap rather than injecting plasma into the inner magnetosphere. As sketched in Figure 6*a*, a convection pattern of the four-cell type [*Burke et al.*, 1979] results, with viscous cells at lower latitudes and lobe cells circulating within the polar caps. The sunward flow segments of the lobe cells contain accelerated auroral particles as described above. These segments were referred to as reclosure cells by *Reiff and Burch* [1985]. Also shown in Figure 6*a* are two merging cells (as described by *Burch et al.* [1985]). These merging cells are added because even for strong northward IMF some low level of merging likely exists that produces open field lines that do not cross

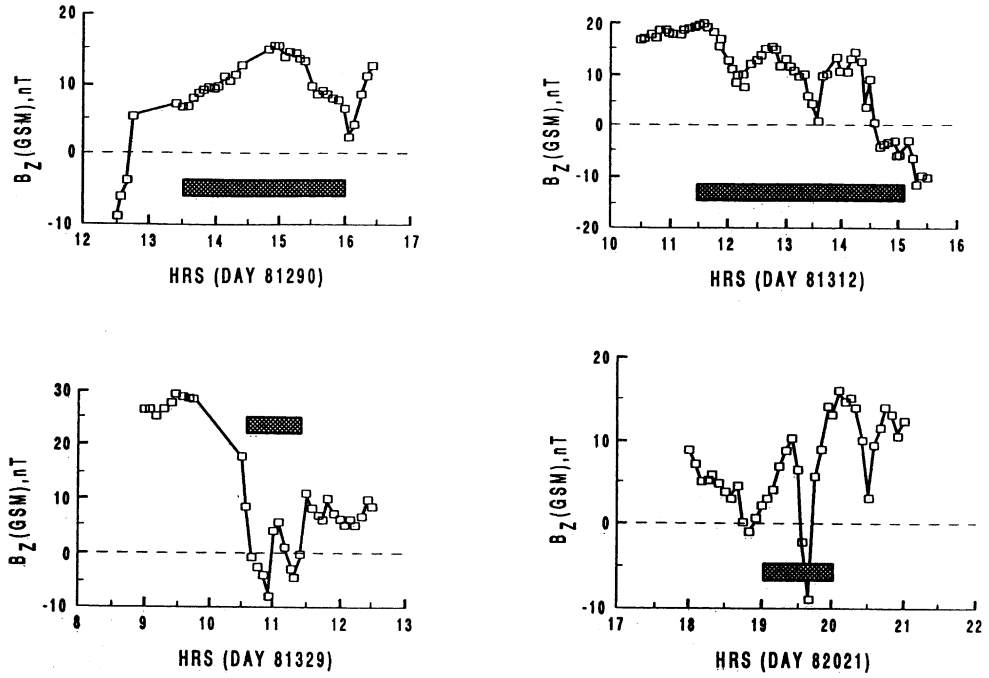


Fig. 4. Five-minute averages of IMF $B_z$ with shaded bars showing times of observation of theta auroras shifted 1 hour earlier to account for the typical travel time from ISEE 3.

the equatorial plane near the Earth and thus can convect directly across the polar caps. The return flow for reconnected field lines of this type would feed into the main auroral oval, through which they return to the dayside. Even for strongly northward IMF, then, there should be a narrow channel of antisunward flow in the central polar cap, and there should be dual transpolar arcs. In fact, every case presented by *Frank et al.* [1986], as well as other published theta arcs [*Elphinstone et al.*, 1990; *Craven et al.*, 1991; *Nielsen et al.*, 1990], shows this dual structure.

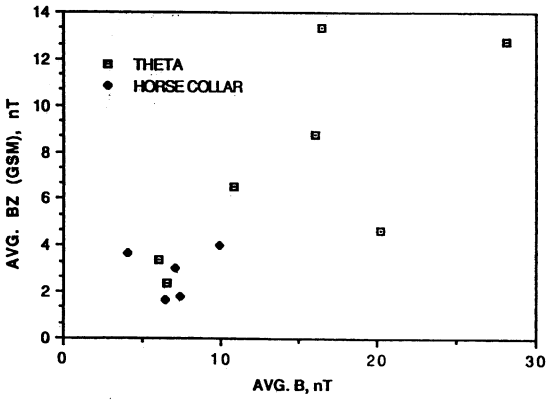


Fig. 5. Average values of IMF $B_z$ versus $B$ for the theta aurora and horse collar aurora observations. Average values were computed over the time interval from 1 hour before the start of the observation period until the end of the period. In the case of ISEE 3 measurements a 1-hour time delay was assumed.

An antisunward flow region between the dual theta arcs would be expected to grow within the polar cap as the IMF takes on weaker northward components, and this growth is the essential feature leading to horse collar auroral configurations in this conceptual model. The sketch in Figure 6*b* depicts the configuration of auroral forms that would be expected for weakly northward IMF. The main auroral oval is sketched simply as a circle, just as in Figure 6*a*, and again is considered to be associated with the large-scale convection reversal of the viscous cell. As shown in Figure 6*b*, for weakly northward IMF the dual polar arcs spread outward into the horse collar aurora or teardrop configuration. As in the strongly northward case of Figure 6*a*, antisunward flow occurs in the dark regions between the oval and the polar arcs and between the polar arcs. For both the strongly northward IMF case of Figure 6*a* and the weakly northward IMF case of Figure 6*b* the polar cap auroral forms lie along convection reversals that separate the lobe cells from the merging cells. Just as for the main auroral oval, the reversal on the duskside involves $\nabla \cdot \mathbf{E} < 0$, while the dawnside reversal involves $\nabla \cdot \mathbf{E} > 0$. Therefore, while particle energization can be explained by induced electric fields, the regions of maximum particle precipitation and acceleration at low altitudes will be determined by the field-aligned current flow into and out of the ionosphere. For a discussion of the multiple convection reversals that occur at the dawnside downward field-aligned current regions, see *Burch et al.* [1976].

## DISCUSSION

Recent magnetospheric mapping results using the Tsyganenko-Usmanov (T-U) 1987 model [*Birn et al.*, 1991; *Elphin-*

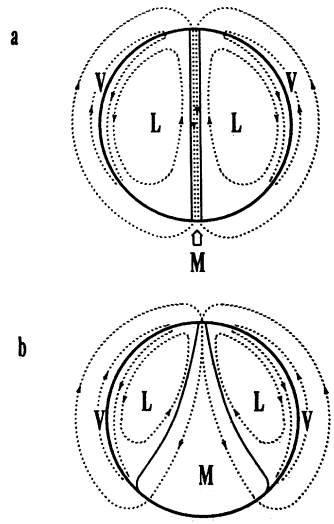


Fig. 6. Sketches of polar cap convection patterns (dotted lines) associated with (*a*) theta auroras and (*b*) horse collar auroras. V, L, and M denote viscous cells, lobe cells, and merging cells, respectively. The solid lines represent auroral forms. The view is looking downward on the northern polar regions, with local noon at the top of each figure.

*stone et al.*, 1991] have shown that during quiet times the open-closed field line boundary has a configuration very similar to the horse collar aurora. *Birn et al.* [1991] defined closed field lines as those that cross the equatorial plane, so the strongly northward IMF merged field lines would be classified as closed even though they extend out into the solar wind. In the *Elphinstone et al.* [1991] study, "code 4" field lines from the region in the dayside polar cap just equatorward of the polar arcs map out to the flanks of the magnetotail. They therefore have the configuration of merged equator-crossing field lines. The total amount of magnetic flux on non-equator-crossing open field lines (the "code 2" field lines of *Elphinstone et al.* [1991]) should increase as the northward IMF components become weaker. Thus a prediction of this conceptual model would be that for strongly northward IMF the region of open field lines in a model such as T-U 1987 would shrink to a narrow channel between two adjacent transpolar theta arcs. The sketch shown in Figure 7 illustrates the closed field lines and the equator-crossing and non-equator-crossing open field lines that are associated with viscous cells, lobe cells, and merging cells, respectively. The sketch assumes that the IMF $y$ and $z$ components vary either in time or across the magnetopause over the range shown by the shaded region in the inset of Figure 7.

As pointed out above, reconnection of the equator-crossing open field lines on the nightside of the polar cap would lead to a reconfiguration or dipolarization of the type normally associated with substorms. However, since the dayside merging site is along the high-latitude magnetopause, there will be sunward flow across the polar cap as the field line is contracting, causing the substorm effects (e.g., auroral particle acceleration and the associated wave emissions) to be channeled across the polar cap rather than into the inner magnetosphere as occurs in substorms. Such substorm-type disturbances in the polar cap were described as the polar substorm by *Craven et al.* [1986]. This channeling of reconnection flows and plasma energization into the polar cap marks the fundamental difference between this model and that of *Kan and Burke* [1985]. In the Kan and Burke model the field lines threading the transpolar arc are essentially on steady state convection with sunward flow in the ionosphere and antisunward flow in the equatorial magnetotail. In that model, since the flux tubes are enlarging and are on steady convection, there is little reason to expect auroral phenomena to be excited within them.

Even with the theta arc configuration, this model predicts a narrow region of antisunward flow associated with low-latitude dayside merging. Therefore there is some small probability of a normal substorm-type disturbance occurring along with the theta arcs, with the substorm effects propagating toward lower latitudes as in normal substorms. In fact, a striking example of such an occurrence has been shown by *Craven et al.* [1991]. Their example appears in Table 1 as the tenth entry.

## SUMMARY

We have presented a conceptual northward IMF merging model based on DE 1 plasma, convection electric field, and wave observations as well as global auroral imaging. The model is capable of explaining several well-known phenomena associated with northward IMF conditions and makes some predictions that can be tested with further observations and models. The model involves dayside merging both at high latitudes on open field lines (the usual northward IMF merging) and at lower latitudes on closed field lines. The ratio between the merged flux produced by the high-latitude merging and the lower-latitude merging increases as the IMF becomes more northward. Reference to Figure 2 of *Crooker* [1979] may be instructive in this regard. As the IMF varies from southward to northward, the merging sites, while

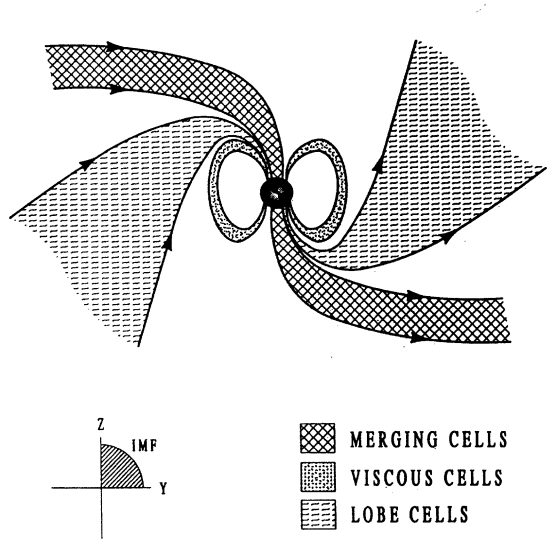


Fig. 7. View from Sun of magnetic flux tubes associated with viscous cells, lobe cells, and merging cells for an IMF that varies within the shaded region of $y$ and $z$ components shown in the inset.

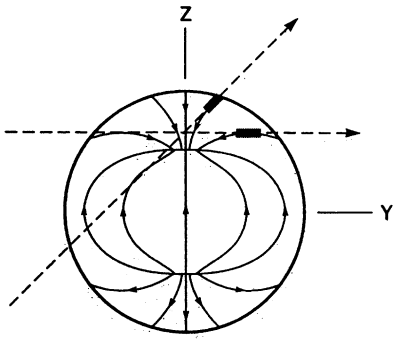


Fig. 8. View from the Sun of magnetic field lines (solid lines) along the magnetopause (with a circular cross section shown by the heavier solid line). IMF magnetic field lines are dashed. Shaded regions are locations of antiparallel merging. (Adapted from *Crooker* [1979].)

generally staying near the cusp, move to successively higher latitudes. Two types of open field lines are produced by the two types of merging: equator crossing and non-equator crossing. Figure 8 illustrates how the two types of open field lines might be formed in the antiparallel merging model of *Crooker* [1979]. Figure 8 combines elements of Figures 1 and 2 of Crooker's paper. We see in Figure 8 that an IMF with $B_x = B_z = 0$ and $B_y > 0$ will merge with closed field lines in the afternoon sector near the cusp, resulting in the transfer of magnetic flux from closed to open field lines. Also shown in Figure 8 is a higher-latitude merging site on open field lines near the afternoon sector cusp for the IMF conditions $B_x = 0$ and $B_y \sim B_z > 0$. For this latter case of stronger IMF $B_z$ positive, the open field lines that are formed cross the equator near the magnetopause. The equator-crossing open field lines have a strong azimuthal component of convection in the ionosphere as the solar wind carries them through the downstream magnetosheath, while the non-equator-crossing open field lines can convect more or less directly over the polar cap, depending on the magnitude of IMB $B_y$. The non-equator-crossing open field lines match the description of open field lines normally used by magnetospheric models.

Upon reconnection in the magnetotail both types of field lines will return toward the Earth with a substorm-type reconfiguration or dipolarization because they will be stretched out much more than the closed field lines that are convected downstream by viscous processes. The main difference is that a reconnected equator-crossing field line will, while contracting to a more dipolar configuration, convect in a generally sunward direction across the polar cap until it becomes the first swept-back field line of the dayside magnetosphere, at which time it will either reconnect with the northward IMF or be convected toward the inner magnetosphere by viscous processes. In the model, weaker northward IMF components lead to polar cap auroras with the horse collar type configuration, while theta arc configurations occur when the IMF is strongly northward. In both cases the major auroral forms lie in regions of closed magnetic flux tubes near convection reversal boundaries. The model further predicts the dual theta arc configuration that is commonly observed by spacecraft imagers. It also predicts sunward convection of closed magnetic flux tubes in the magnetotail regions that map from the polar arcs, which can be interpreted as the "magnetotail bifurcation" suggested by *Frank et al.* [1982] since these regions are bounded by antisunward convecting open field lines.

*Acknowledgments.* We thank C. Gurgiolo and M. Muller of SwRI and Ann Persoon of the University of Iowa for assistance with computer analysis of the DE 1 data. Helpful discussions with Bill Burke, Joe Kan, Pat Reiff, and Chin Lin are gratefully acknowledged. The IMP 8 (R. P. Lepping, PI) and the ISEE 3 (E. J. Smith, PI) data were provided by the National Space Science Data Center. ISEE 1 data were kindly provided by C. T. Russell. At UTSA this work was supported by NASA grants NAGW-1254 and NAGW-1663, NSF grant ATM-89-42746, and at SwRI by NASA contract NAS5-33030, and at the University of Iowa by NASA grant NAG5-483. Initial participation by J.D.C. occurred while he was at the University of Iowa. Research at the University of Alaska Fairbanks was supported in part by NASA grant NAGW-2735.

The Editor thanks R. D. Elphinstone and another referee for their assistance in evaluating this paper.

## REFERENCES

Birn, J., E. W. Hones, Jr., J. D. Craven, L. A. Frank, R. D. Elphinstone, and D. P. Stern, On open and closed field line regions in Tsyganenko's field model and their possible associations with horse collar auroras, *J. Geophys. Res.*, *96*, 3811–3817, 1991.

Blomberg, L. G., and G. T. Marklund, High-latitude convection patterns for various large-scale field-aligned current configurations, *Geophys. Res. Lett.*, *18*, 717–720, 1991.

Burch, J. L., W. Lennartsson, W. B. Hanson, R. A. Heelis, J. H. Hoffman, and R. A. Hoffman, Properties of spikelike shear flow reversals observed in the auroral plasma by Atmosphere Explorer C, *J. Geophys. Res.*, *81*, 3886–3896, 1976.

Burch, J. L., et al., IMF $B_y$-dependent plasma flow and Birkeland currents in the dayside magnetosphere, 1, Dynamics Explorer observations, *J. Geophys. Res.*, *90*, 1577–1593, 1985.

Burke, W. J., M. C. Kelley, R. C. Sagalyn, M. Smiddy, and S. T. Lai, Polar cap electric field structures with a northward interplanetary magnetic field, *Geophys. Res. Lett.*, *6*, 21–24, 1979.

Craven, J. D., L. A. Frank, C. T. Russell, E. J. Smith, and R. P. Lepping, The global auroral response to magnetospheric compressions by shocks in the solar wind: Two case studies, in *Solar Wind–Magnetospheric Coupling*, edited by Y. Kamide and J. A. Slavin, pp. 367–380, Terra Scientific, Tokyo, 1986.

Craven, J. D., J. S. Murphree, L. A. Frank, and L. L. Cogger, Simultaneous optical observations of transpolar arcs in the two polar caps, *Geophys. Res. Lett.*, *18*, 2297–2300, 1991.

Crooker, N. U., Dayside merging and cusp geometry, *J. Geophys. Res.*, *84*, 951–959, 1979.

Delcourt, D. C., J. A. Sauvaud, and A. Pedersen, Dynamics of single-particle orbits during substorm expansion phase, *J. Geophys. Res.*, *95*, 20,853–20,865, 1990.

Dungey, J. W., Interplanetary magnetic field and the auroral zones, *Phys. Rev. Lett.*, *6*, 47, 1961.

Elphinstone, R. D., K. Jankowska, J. S. Murphree, and L. L. Cogger, The configuration of the auroral distribution for interplanetary magnetic field $B_z$ northward, 1, IMF $B_x$ and $B_y$ dependencies as observed by the Viking satellite, *J. Geophys. Res.*, *95*, 5791–5804, 1990.

Elphinstone, R. D., D. Hearn, J. S. Murphree, and L. L. Cogger, Mapping using the Tsyganenko long magnetospheric model and its relationship to Viking auroral images, *J. Geophys. Res.*, *96*, 1467–1480, 1991.

Fairfield, D. H., and J. D. Scudder, Polar rain: Solar coronal electrons in the Earth's magnetosphere, *J. Geophys. Res.*, *90*, 4055–4068, 1985.

Frank, L. A., J. D. Craven, J. L. Burch, and J. D. Winningham, Polar views of the Earth's aurora with Dynamics Explorer, *Geophys. Res. Lett.*, *9*, 1001–1004, 1982.

Frank, L. A., et al., The theta aurora, *J. Geophys. Res.*, *91*, 3177–3224, 1986.

Hoffman, R. A., M. Sugiura, N. C. Maynard, R. M. Candey, J. D. Craven, and L. A. Frank, Electrodynamic patterns in the polar

region during periods of extreme magnetic quiescence, *J. Geophys. Res.*, *93*, 14,515–14,541, 1988.

Hones, E. W., Jr., J. D. Craven, L. A. Frank, D. S. Evans, and P. T. Newell, The horse-collar aurora: A frequent pattern of the aurora in quiet times, *Geophys. Res. Lett.*, *16*, 37–40, 1989.

Israelevich, P. L., The change of magnetospheric configuration due to cross-tail current disruption and its possible relation to the appearance of θ-aurora, *Planet. Space Sci.*, *38*, 1361–1366, 1990.

Jankowska, K., R. D. Elphinstone, J. S. Murphree, L. L. Cogger, D. Hearn, and G. Marklund, The configuration of the auroral distribution for interplanetary magnetic field $B_z$ northward, 2, Ionospheric convection consistent with Viking observations, *J. Geophys. Res.*, *95*, 5805–5816, 1990.

Kan, J. R., and W. J. Burke, A theoretical model of polar cap auroral arcs, *J. Geophys. Res.*, *90*, 4171–4177, 1985.

Lassen, K., The quiet time pattern of auroral arcs as a consequence of magnetospheric convection, *Geophys. Res. Lett.*, *6*, 777–780, 1979.

Lockwood, M., M. O. Chandler, J. L. Horwitz, J. H. Waite, Jr., T. E. Moore, and C. R. Chappell, The cleft ion fountain, *J. Geophys. Res.*, *90*, 9736–9748, 1985.

Maezawa, K., Magnetospheric convection induced by the positive and negative z components of the interplanetary magnetic field: Quantitative analysis using polar cap magnetic records, *J. Geophys. Res.*, *81*, 2289–2303, 1976.

Murphree, J. S., C. D. Anger, and L. L. Cogger, The instantaneous relationship between polar cap and oval auroras at times of northward interplanetary magnetic field, *Can. J. Phys.*, *60*, 349–356, 1982.

Nielsen, E., J. D. Craven, L. A. Frank, and R. A. Heelis, Ionospheric flows associated with a transpolar arc, *J. Geophys. Res.*, *95*, 21,169–21,178, 1990.

Obara, T., M. Kitayama, T. Mukai, N. Kaya, J. S. Murphree, and L. L. Cogger, Simultaneous observations of Sun-aligned polar cap arcs in both hemispheres by EXOS-C and Viking, *Geophys. Res. Lett.*, *15*, 713–716, 1988.

Persoon, A. M., D. A. Gurnett, W. K. Peterson, J. H. Waite, Jr., J. L. Burch, and J. L. Green, Electron density depletions in the nightside auroral zone, *J. Geophys. Res.*, *93*, 1871–1895, 1988.

Reiff, P. H., and J. L. Burch, IMF $B_y$-dependent plasma flow and Birkeland currents in the dayside magnetosphere, 2, A global model for northward and southward IMF, *J. Geophys. Res.*, *90*, 1595–1609, 1985.

Rich, F. J., and M. S. Gussenhoven, The absence of region 1/region 2 field-aligned currents during prolonged quiet times, *Geophys. Res. Lett.*, *14*, 689–692, 1987.

Song, P., and C. T. Russell, Model of the formation of the low-latitude boundary layer for strongly northward interplanetary magnetic field, *J. Geophys. Res.*, *97*, 1411–1420, 1992.

Tsyganenko, N. A., Global quantitative models of the geomagnetic field in the cislunar magnetosphere for different disturbance levels, *Planet. Space Sci.*, *35*, 1347–1358, 1987.

Zanetti, L. J., T. A. Potemra, T. Iijima, W. Baumjohann, and P. F. Bythrow, Ionospheric and Birkeland current distributions for northward interplanetary magnetic field: Inferred polar convection, *J. Geophys. Res.*, *89*, 7453–7458, 1984.

Zhu, L., and J. R. Kan, Relationships between four-cell and distorted two-cell convection patterns during northward IMF, *Geophys. Res. Lett.*, *17*, 2325–2328, 1990.

J. L. Burch, Southwest Research Institute, P. O. Drawer 28510, San Antonio, TX 78228-0510.

J. D. Craven, Geophysical Institute, University of Alaska, Fairbanks, AK 99775.

L. A. Frank and D. A. Gurnett, Department of Physics and Astronomy, University of Iowa, Iowa City, IA 52242.

N. A. Saflekos, Division of Earth and Physical Sciences, University of Texas at San Antonio, San Antonio, TX 78285.

(Received March 6, 1992;
revised June 16, 1992;
accepted June 16, 1992.)